**SOS1 and KSR1 modulate MEK inhibitor responsiveness to target resistant cell populations based on PI3K and KRAS mutation status**

Brianna R. Daley[1,2], Heidi M. Vieira[1,3], Chaitra Rao[3,4], Jacob M. Hughes[2], Dianna H. Huisman[3], Deepan Chatterjee[5], Nancy E. Sealover[2], Katherine Cox[2], James W. Askew[3], Zaria M. Beckley[2], Robert A. Svoboda[6], Kurt W. Fisher[6], Robert E. Lewis[3*], and Robert L. Kortum[2*]

[1]These authors contributed equally to this paper

[2]Department of Pharmacology and Molecular Therapeutics, Uniformed Services University of the Health Sciences, Bethesda, MD

[3]Eppley Institute for Research in Cancer and Allied Diseases, University of Nebraska Medical Center, Omaha, NE

[4]Current address: Wells Center for Pediatric Research, Indiana University School of Medicine, Indianapolis, IN

[5]Integrative Physiology and Molecular Medicine, University of Nebraska Medical Center, Omaha, NE

[6]Department of Pathology and Microbiology, University of Nebraska Medical Center, Omaha, NE

*Corresponding Authors

Robert E. Lewis
Eppley Institute
986805 Nebraska Medical Center
Omaha, NE. 68198-6805
**Email:** rlewis@unmc.edu

Robert L. Kortum
Uniformed Services University of the Health Sciences
4301 Jones Bridge Rd
Bldg C, Rm C2027
Bethesda, MD 20814
**Email:** robert.kortum@usuhs.edu

**Author Contributions:** BRD, HMV, REL, and RLK designed the experiments and analyzed the data; BRD, HMV, and RLK performed most of the experiments; CR assisted with clonogenicity and resistance studies in *KSR1* KO cells; JMH assisted with synergy studies, *in vitro* ELDAs, and resistance studies; NES, KC, and ZMB assisted with in vitro ELDAs and signaling studies; DHH, DC, and JWA assisted with *in vivo* ELDA studies; CR, RAS and KWF assisted with *KSR1* genomic targeting. BRD, HMV, REL, and RLK wrote the manuscript, NES edited the manuscript.

**Competing Interest Statement:** The Kortum laboratory receives funding from Boehringer Ingelheim to study SOS1 as a therapeutic target in *RAS*-mutated cancers.

**Classification:** Biological Sciences; cell biology

**Keywords:** RAS, SOS1, KSR1, therapeutic resistance, KRAS

**Abstract**

KRAS is the most commonly mutated oncogene. Targeted therapies have been developed against mediators of key downstream signaling pathways, predominantly components of the RAF/MEK/ERK kinase cascade. Unfortunately, single-agent efficacy is limited both by intrinsic and acquired resistance. Survival of drug-tolerant persister cells within the heterogeneous tumor population and/or acquired mutations that reactivate receptor tyrosine kinase (RTK)/RAS signaling can lead to outgrowth of tumor initiating cells (TICs) and drive therapeutic resistance. Here, we show that targeting the key RTK/RAS pathway signaling intermediates SOS1 or KSR1 both enhanced the efficacy of, and prevented resistance to, the MEK inhibitor trametinib in *KRAS*-mutated lung (LUAD) and colorectal (COAD) adenocarcinoma cell lines depending on the specific mutational landscape. The SOS1 inhibitor BI-3406 enhanced the efficacy of trametinib and prevented trametinib resistance by targeting TICs in $KRAS^{G12}$- or $KRAS^{G13}$-mutated LUAD and COAD cell lines that lacked *PIK3CA* co-mutations. Cell lines with $KRAS^{Q61}$ and/or *PIK3CA* mutations were insensitive to combination therapy with trametinib and BI-3406. In contrast, deletion of the RAF/MEK/ERK scaffold protein *KSR1* prevented drug-induced TIC upregulation and restored trametinib sensitivity across all tested *KRAS* mutant cell lines in both *PIK3CA*-mutated and *PIK3CA* wildtype cancers. Our findings demonstrate that vertical targeting of RTK/RAS signaling is an effective strategy to target *KRAS*-mutated cancers, but the specific combination is dependent both on the specific KRAS mutant and underlying co-mutations. Thus, selection of optimal therapeutic

combinations in *KRAS*-mutated cancers will require a detailed understanding of functional dependencies imposed by allele-specific KRAS mutations.

**Significance Statement**

We provide an experimental framework for evaluating both adaptive and acquired resistance to RAS pathway-targeted therapies and demonstrate how vertical inhibition of RAS signaling enhances the effectiveness of MEK inhibitors in *KRAS*-mutated cancer cells. Targeting RAS pathway signaling intermediates SOS1 or KSR1 inhibited tumor initiating cell formation to prevent trametinib resistance. The contribution of either effector to resistance was dependent upon the mutational landscape: SOS1 inhibition synergized with trametinib $KRAS^{G12/G13}$-mutated cells expressing WT PI3K but not in $KRAS^{Q61}$-mutated cells or if *PIK3CA* is mutated. *KSR1* deletion is effective in cells that are unresponsive to SOS1 inhibition. These data show that optimal therapeutic combinations require a detailed understanding of functional dependencies imposed both by allele-specific *KRAS* mutations and specific co-mutations.

**Main Text**

**Introduction**

RAS proteins are encoded by three paralogs, KRAS, NRAS, and HRAS, which are, collectively, the most frequently mutated oncogene in cancer (1, 2). Among these paralogs, KRAS is the most commonly mutated, found predominantly in pancreas adenocarcinoma (PDAC) (95%), lung adenocarcinoma (LUAD) (30-40%), and colorectal adenocarcinoma (COAD) (45-50%) (3). KRAS is commonly mutated at one of three mutational hotspots, G12, G13, or Q61 (4); mutation of one of these sites alters KRAS GTP/GDP cycling leading to increased KRAS-GTP loading and hyperactivation of downstream effectors including the pro-proliferative RAF/MEK/ERK kinase cascade. The RAF/MEK/ERK kinase cascade is the critical driver of proliferation in *KRAS*-mutated cancers (5-9), and multiple small molecule inhibitors of each kinase have been evaluated in *KRAS*-mutated cancers (10). Of these, the MEK inhibitors trametinib and selumetinib are among the most promising agents (11, 12). Unfortunately, single-agent treatment with MEK inhibitors is largely ineffective in *KRAS*-mutated cancers due to both intrinsic (adaptive) and acquired resistance. Intrinsic resistance occurs due to the presence of pre-existing mechanisms that render tumor cells insensitive to that specific therapeutic intervention (13). For MEK inhibitors, intrinsic resistance is driven both by relief of ERK-dependent negative feedback of RTK−SOS−WT RAS−PI3K signaling (14-18) and compensatory ERK reactivation (5, 19, 20). Thus, either broad inhibition of RTK rebound signaling and/or deep inhibition of MEK/ERK signaling may be required to enhance the efficacy of MEK inhibitors to treat *KRAS*-mutated cancers (18, 21, 22).

Even if one is able to overcome intrinsic/adaptive resistance, treatment failure can also occur via acquired resistance, where resistance-conferring mutations, phenotypes, or shifts in oncogenic signaling that occur under selective pressure lead to

tumor outgrowth after an initial period of drug responsiveness (13, 21). *KRAS*-mutated cancer cells treated with MEK inhibitors are capable of surviving targeted treatments by entering a near quiescent state (5, 23), becoming drug-tolerant persisters (DTPs) (21). DTPs exhibit subpopulations of highly plastic cells with altered metabolic and drug efflux properties (21, 24) also known as tumor initiating cells (TICs). TICs exhibit stem-like properties, can self-renew and divide asymmetrically to give rise to additional cell types within the tumor, and may represent the sanctuary population within the bulk tumor responsible for treatment failure and recurrence (25, 26). In colorectal cancer, MEK inhibition may increase the TIC population through promotion of stem-like signaling pathways (27) and targeting TIC emergence may be required to circumvent acquired resistance.

*KRAS*-mutated cancers are addicted to RTK/RAS signaling, and combination therapeutic strategies that vertically inhibit RTK/RAS/effector signaling represents an attractive approach to limiting MEK inhibitor-induced rebound RTK−PI3K signaling and compensatory ERK reactivation in *KRAS*-mutated cancers (5, 14-20). Upstream of RAS, the RAS guanine nucleotide exchange factors (RasGEFs) SOS1 and SOS2 regulate RTK-stimulated RAS activation and represent a key 'stoichiometric bottleneck' for RTK/RAS pathway signaling (28). *SOS2* deletion synergizes with trametinib to inhibit anchorage-independent survival in *KRAS*-mutated cancer cells (18), but only in cells with WT *PIK3CA*. While no SOS2 inhibitors have been developed to date, multiple groups have developed SOS1 inhibitors with the goal of using these to treat RTK/RAS mutated cancers (29-35). The most well characterized SOS1 inhibitor, BI-3406, has modest single-agent efficacy in *KRAS*-mutated cells but enhanced the efficacy of the MEK inhibitor trametinib in KRAS-mutated xenografts (32). BI-3406 activity is RAS

codon-specific, killing cells harboring *KRAS*$^{G12}$ and *KRAS*$^{G13}$ mutations that are dependent upon activation by GEFs, but not cells harboring *KRAS*$^{Q61}$mutations. Mutation of Q61 dramatically reduces intrinsic hydrolysis compared to either G12 or G13 mutations, promoting GEF-independent signaling (36, 37).

Downstream of RAS, Kinase Suppressor of RAS 1 (KSR1) is a molecular scaffold for the RAF/MEK/ERK kinase cascade that controls the intensity and duration of ERK signaling to dictate cell fate (38-40). While KSR1 is required for mutant RAS-driven transformation (38) and tumorigenesis (41), it is dispensable for normal growth and development (41, 42). KSR1 signaling can regulate responses to RAS/MAPK targeted therapies. KSR1 expression level correlates with resistance to the KRAS$^{G12C}$ inhibitor sotorasib in *KRAS*$^{G12C}$-mutated lung adenocarcinoma (LUAD) (43) and stabilizing the KSR inactive state enhances MEK inhibitor effectiveness (44).

Here we demonstrate that vertical inhibition of RTK/RAS signaling is a viable strategy to both enhance the efficacy of, and delay resistance to, the MEK inhibitor trametinib in *KRAS*-mutated cancer cells, but the optimal co-targeting strategy is dependent on both the specific KRAS allelic mutation and the presence of *PIK3CA* co-mutations. In *KRAS*$^{G12}$ and *KRAS*$^{G13}$-mutated LUAD and COAD cells, the SOS1 inhibitor BI-3406 synergistically enhanced trametinib efficacy and prevented the development of trametinib resistance by targeting TICs. These effects were lost in *KRAS*$^{Q61}$-mutated cells or if *PIK3CA* is mutated. In contrast, *KSR1* knockout (KO) limited TIC survival and trametinib resistance in both *KRAS*$^{Q61}$-mutated cells and in *KRAS*-mutated COAD cells with *PIK3CA* co-mutations in an ERK-dependent manner. Thus, selection of optimal

therapeutic combinations in *KRAS*-mutated cancers will require a detailed understanding of functional dependencies imposed by allele-specific KRAS mutations.

## Results

**SOS1 inhibition synergizes with trametinib to prevent rebound signaling in *KRAS$^{G12}$/PIK3CA$^{WT}$*-mutated LUAD cells.** BI-3406 is a potent, selective SOS1 inhibitor previously shown to reduce 3D proliferation of *KRAS$^{G12/G13}$*-mutated, but not *KRAS$^{Q61}$*-mutated, cell lines as a single agent and to enhance the efficacy of trametinib in *KRAS*-mutated xenografts (32). To characterize the extent to which BI-3406 enhances the effectiveness of trametinib, we treated a panel of 3D spheroid cultured *KRAS*-mutated LUAD cell lines with increasing doses of BI-3406 and/or trametinib in a 9x9 matrix of drug combinations and assessed for synergistic killing after 96 hours by Bliss Independence (Fig. 1A). We found that in *KRAS$^{G12X}$*-mutated cell lines H727 (G12V), A549 (G12S), and H358 (G12C), SOS1 inhibition markedly enhanced the efficacy of trametinib at or below the $EC_{50}$ for trametinib (Fig. 1A) and showed a high excess over Bliss (EOB) across the treatment matrix (Fig. 1B).

As a single agent, the effectiveness of trametinib is blunted by rapid induction of RTK/PI3K signaling followed by rebound ERK activation due, in part, to loss of ERK-dependent negative feedback signaling (14, 22, 45). BI-3406 inhibited both the trametinib-induced increase in PI3K/AKT activation and rebound ERK activation in *KRAS$^{G12V}$*-mutated H727 cells (Fig. 1C), suggesting that SOS1 inhibition blocks PI3K-dependent adaptive resistance to MEK inhibitors. Consistent with this hypothesis, SOS1 inhibition did not synergize with trametinib (Fig. 1 A-B) or inhibit rebound signaling (Fig. S1) in *KRAS$^{G12X}$*-mutated LU99A cells that harbor a *PIK3CA* co-mutation, further enhancing the argument that SOS1 enhances trametinib efficacy by inhibiting RTK/PI3K

rebound signaling. SOS1 inhibition also failed to synergize with trametinib (Fig. 1 A-B) and inhibit rebound signaling (Fig. S1) in four different *KRAS*$^{Q61}$-mutated LUAD cell lines regardless of *PIK3CA* mutation status, confirming previous studies that SOS1 inhibition is only effective in *KRAS*-mutated cancer cells where mutant KRAS actively cycles between the GTP and GDP-bound state (32) (KRAS$^{G12/G13}$ mutants), but not in KRAS$^{Q61}$ mutants where the extremely low levels of GTP hydrolysis make them RASGEF independent (Fig. 1D).

**Combination therapy with MEK and SOS1 inhibition targets trametinib-induced TIC outgrowth.** Single agent therapy with EGFR Tyrosine Kinase Inhibitors increases TIC populations in NSCLC (46). MEK inhibitors similarly expand TIC populations in *KRAS*-mutated LUAD cells (Fig. 2). MEK inhibitors trametinib and selumetinib increased ALDH staining in H727 (G12V) (Fig. 2A), A549 (G12S) and H358 (G12C) (Fig. S2A) *KRAS*-mutated *PIK3CA*$^{WT}$ cells. Increased ALDH staining is indicative of an enhanced presence of TICs (47-49). We used Extreme Limiting Dilution Analysis (ELDA) in H727, A549, and H358 cells to assess spheroid growth in 96-well ultra-low attachment plates and determine the frequency of TICs. ELDAs were performed 72 hours after selumetinib or trametinib treatment and assessed after 7-10 days for TIC outgrowth. ELDAs demonstrated a 2-3-fold significant increase in TIC frequency in MEK-inhibitor treated cells in comparison to untreated cells (Fig. 2B).

SOS1 inhibition was effective in blocking adaptive resistance and enhancing the efficacy of trametinib (Fig. 1C), leading us to assess whether *SOS1* KO would be able to kill persister cells in *KRAS*-mutated LUAD cells. Compared to NT control cells, *SOS1* KO caused a 3-5-fold significant decrease in TIC frequency in *KRAS*$^{G12X}$-mutated/*PIK3CA*$^{WT}$

cells (Fig. 2C). SOS1 inhibition with BI-3406 decreases TIC frequency in a dose-dependent manner, with the greatest effect found at 300 nM in H727 (G12V) (Fig. 2D) and A549 (G12S) cells (Fig. S2B). Since SOS1 was required for TIC survival, we hypothesized that SOS1 inhibition would also limit the survival of the increased TICs present following MEK inhibition with trametinib. To test this hypothesis, we pre-treated cells with two doses of trametinib (Fig. 2E) or selumetinib (Fig. S2C) and used these cells for ELDAs plated with either media or BI-3406. We found that in H727, A549, and H358 cells, SOS1 inhibition targeted and significantly decreased the MEK-induced increase in TIC frequency, causing a 5-10-fold significant decrease in TICs in MEK-inhibitor treated cells (Fig. 2E and S2C). These findings support our hypothesis that BI-3406 can be used to enhance the efficacy of trametinib and prevent the development of resistance in the presence of *KRAS*$^{G12/G13}$-mutated LUAD cells without a *PIK3CA* mutation.

*SOS1* KO and drug sensitivity is dependent upon the mutational profile of LUAD cells. *SOS1* KO had no effect on TIC frequency in *KRAS*$^{G12X}$/*PIK3CA*$^{MUT}$ (LU99A) cells or *KRAS*$^{Q61X}$-mutated cells that are either *PIK3CA* wildtype (Calu6) or *PIK3CA* mutant (H460) (Fig. 2C). In *KRAS*$^{Q61K}$/*PIK3CA*$^{WT}$ Calu6 cells, trametinib increased TIC frequency 2-3-fold, however, trametinib did not cause a significant increase in TICs in LUAD cells harboring a *PIK3CA* mutation (LU99A, H460) (Fig. 2E), suggesting that mutations within the PI3K/AKT pathway and/or trametinib-induced RTK-PI3K signaling may drive LUAD TIC outgrowth.

***KSR1* KO restores trametinib responsiveness and inhibits TIC survival in *KRAS/PIK3CA* co-mutated LUAD cells.** The RAF/MEK/ERK scaffold protein, KSR1, is

a positive regulator of ERK-dependent signaling in *RAS*-mutant cancers, but dispensable to the growth of untransformed cells and could therefore be a promising therapeutic target downstream of oncogenic RAS (38, 40, 50). Structural analysis reveals that trametinib binds to the MEK-KSR complex (44). In *KRAS*$^{Q61X}$/*PIK3CA*$^{MUT}$ H460 cells, RAS activation is less dependent on upstream signaling compared to *KRAS*$^{G12/G13}$-mutated cells, and SOS1 inhibition did not synergize with trametinib (Fig. 1A-B), inhibit rebound PI3K or ERK signaling (Fig. S1), or suppress TICs (Fig. 2E). We sought to determine whether inhibition of RAF/MEK/ERK signaling downstream of RAS via KSR1 disruption affects TIC survival and trametinib sensitivity in *KRAS*$^{Q61H}$/*PIK3CA*$^{MUT}$ H460 LUAD cells. Since TIC frequencies in H460 cells were very high *in vitro* (Fig. 2), we tested the effect of KSR1 deletion on TIC frequency *in vivo*. CRISPR/Cas9-mediated knockout of *KSR1* reduced TIC-frequency 4-fold by *in vivo* ELDA, demonstrating that KSR1 regulates the TIC populations in H460 cells (Fig. 3A). *KSR1* KO further sensitized H460 cells to trametinib and selumetinib, significantly enhancing the potency as assessed by $EC_{50}$ of each MEK inhibitor under both 2D (adherent) and 3D (spheroid) culture conditions (Fig. 3B-C and S3). In trametinib treated cells, *KSR1* KO both synergized with trametinib in a dose-dependent manner to cause deep ERK inhibition (Fig. 3C) and inhibited compensatory ERK reactivation (Fig. 3D) to limit adaptive resistance. These data demonstrate that inhibition of signaling distal to RAS depletes TICs and restores trametinib responsiveness in Q61 *RAS*-mutant and *PIK3CA*-mutant LUAD cells, where inhibition of signaling proximal to RAS fails.

**In COAD, *KSR1* KO prevents trametinib-induced TIC increase in cells unresponsive to SOS1 inhibition**. While *KRAS/PIK3CA* co-mutations are relatively

rare in LUAD, they commonly co-occur in COAD, with approximately one third of *KRAS*-mutated COADs harboring co-existing *PIK3CA* mutations. We sought to test the extent to which the *KRAS/PIK3CA* genotype sensitivity to SOS1 and KSR1 ablation we observed in LUAD would remain true in COAD. Therefore, we generated CRISPR/Cas9-mediated knockout of *KSR1* in four COAD cell lines with varying *PIK3CA* status: SW480 ($KRAS^{G12C}/PIK3CA^{WT}$) LoVo ($KRAS^{G13D}/PIK3CA^{WT}$), LS174T ($KRAS^{G12D}/PIK3CA^{MUT}$), and T84 ($KRAS^{G13D}/PIK3CA^{MUT}$). *In vitro* ELDAs performed with *KSR1* KO in the four COAD cell lines demonstrated a 2-3-fold significant decrease in TIC-frequency compared to NT cells. Further, *KSR1* KO prevented the trametinib-induced increase in TIC in the four COAD cell lines (Fig. 4), demonstrating that the KSR1 effect on TICs in COAD is independent of *PIK3CA* mutational status. Further, treatment with BI-3406 in NT cells prevented trametinib-induced TIC increase in the cell lines with wildtype *PI3KCA* status (SW480 and LoVo), but not in $PIK3CA^{MUT}$cell lines (LS174T and T84), consistent with our LUAD findings (Fig. 2E). In *KSR1* KO cells, combination of trametinib with BI-3406 did not further affect TIC frequency, concordant with SOS1 acting upstream of KSR1 in the RTK/RAS pathway (Fig. S4).

**KSR1 regulation of TIC survival in *KRAS*-mutated COAD is dependent on interaction with ERK.** KSR1 mediates ERK-dependent signaling in transformed and untransformed cells via direct interaction between its DEF domain and ERK (40, 51, 52). A KSR1 transgene deficient in binding ERK due to engineered mutation in the DEF-domain, $KSR1^{AAAP}$ (40), was expressed in *KSR1* KO colorectal adenocarcinoma cell line HCT116 ($KRAS^{G13D}/PIK3CA^{MUT}$) (Fig. 5A). Expression of $KSR1^{AAAP}$ in *KSR1* KO cells failed to rescue ALDH activity, single cell clonogenicity, or anchorage-independent growth by soft agar assay to the level observed with wildtype KSR1 addback,

demonstrating the necessity of ERK interaction on KSR1 regulation of TICs (Fig. 5B-D). To assess KSR1 function in a preclinical setting, an *in vivo* limiting dilution analysis was performed. Notably, a 70-fold decrease in the proportion of TICs was found in the *KSR1* KO cells compared to those with NT cells, demonstrating the significant impact of KSR1 on TICs in COAD (Fig. 5E).

**SOS1 and KSR1 disruption prevent trametinib resistance in *KRAS*-mutated cells.** To assess the effect of SOS1 and KSR1 disruption on outgrowth of trametinib-resistant cells, we utilized multi-well *in situ* resistance assays (53) in which cells are grown on a 96-well plate and treated with trametinib alone or in combination with BI-3406. Wells are scored twice weekly to assess for 50% confluency or more to determine the presence of resistance. Of the five LUAD cell lines tested, SOS1 inhibition with BI-3406 prevented outgrowth of trametinib-resistant cells in ($KRAS^{G12V}/PI3KCA^{WT}$) and H358 cells ($KRAS^{G12C}/PI3KCA^{WT}$), but not in LUAD cell lines with either a *PIK3CA* co-mutation (LU99A), $KRAS^{Q61}$ mutation (Calu6), or both (H460) (Fig. 6A-E). In contrast, *KSR1* KO was able to prevent outgrowth of trametinib-resistant cells in H460 LUAD cells (Fig. 6F) and in the HCT116 ($KRAS^{G13D}/PIK3CA^{MUT}$) COAD cell line (Fig. 6G). To determine whether interaction with ERK was necessary for the KSR1 effect on trametinib resistance, we further tested whether expression of ERK-binding mutant $KSR1^{AAAP}$ in *KSR1* KO cells could rescue trametinib-resistant outgrowth. $KSR1^{AAAP}$ partially restored outgrowth relative to *KSR1* KO cells while wildtype KSR1 completely restored outgrowth (Fig. 6F), suggesting KSR1 interaction with ERK affects trametinib resistance but may be occurring in combination with other KSR1-dependent effects.

**Discussion**

Within the RTK/RAS pathway, there is a hierarchical dependency of downstream signaling pathways depending upon the specific RAS mutation, with KRAS predominantly signaling downstream to the RAF/MEK/ERK pathway (9, 54-57). Thus, targeting MEK is an attractive option for treating patients with *KRAS*-mutated tumors. Unfortunately, trametinib monotherapy is largely ineffective due to both the loss of ERK-dependent negative feedback control of RTKs (adaptive resistance (5, 14-19, 21, 22)) as well as the subsequent selection of tumor initiating cells through therapeutic-pressure over-time (acquired resistance (5, 13, 21, 23)). Previous studies designed to identify MEK inhibitor co-targets have identified combinations that can overcome adaptive resistance (22, 32, 58, 59), but have not examined the extent to which these combinations may prevent the acquisition of acquired resistance. Here, we provide an experimental framework for evaluating both adaptive and acquired resistance to RTK/RAS pathway targeted therapies, and use this framework to show that vertical inhibition of RTK/RAS signaling can enhance the overall effectiveness of MEK inhibitors in *KRAS*-mutated cancer cells.

Essential to building this framework is having reliable experimental approaches that model each step of the evolution of a cancer cell due to therapeutic pressure and then to use this framework when assessing novel drug combinations. The ideal drug combination would (i) enhance the efficacy of an oncogene-targeted therapy to overcome intrinsic/adaptive resistance, (ii) limit the survival of TICs, which are the subset of drug-tolerant persister (DTP) cells capable of driving adaptive resistance, and (iii) delay the onset of and/or block the development of resistant cultures. To examine the extent to which combination therapies enhance the efficacy of an oncogene-targeted therapy to overcome intrinsic/adaptive resistance in *KRAS*-mutated cancers, we

assessed drug-drug synergy in 3D spheroid cultures (Fig. 1). 3D culture conditions are essential to the assessment of drug-drug synergy in RTK/RAS-mutated cancers. *KRAS*-mutated cell lines originally classified as KRAS-independent in 2D adherent culture (60-64) require KRAS expression (65-68) or become sensitized to $KRAS^{G12C}$ inhibitors (69) in 3D culture conditions. Further, inhibition or deletion of proximal RTK signaling intermediates SOS1 (31, 32, 70), SOS2 (18, 57), and SHP2 (22, 70-72) inhibit proliferation of RTK/RAS mutated cancers and synergize with therapies targeting the RTK/RAS pathway, but only under 3D culture conditions. To assess enrichment of TICs within the therapy-tolerant persister cell population and the extent to which combination therapies can block this enrichment, we perform extreme limiting dilution assays (ELDAs) (9, 73) in 3D culture conditions (Figs. 2-4) that allow us to estimate the frequency of TICs within a cell population and show increased TIC frequency when *KRAS*-mutated cells are pre-treated with trametinib. This enrichment of TICs upon trametinib treatment confirms that beyond adaptive resistance, there is likely underlying molecular heterogeneity in *KRAS*-mutated cancers associated with drug-tolerant persister (DTP) cells that allow for acquired resistance to trametinib over time. To assess the extent to which therapeutic combinations limit the development of acquired resistance, we use *in situ* resistance assays (ISRAs) that our laboratory developed as a hybrid approach that combines elements of time-to-progression assays (59, 74) and cell outgrowth assays described originally by the Jänne laboratory (75, 76). These longitudinal studies of acquired resistance act as a cell-culture surrogate of multi-individual trials that should be performed prior to testing therapeutic combinations *in vivo* (53).

Using this framework, we found SOS1 inhibition using BI-3406 both enhanced the efficacy of trametinib by preventing reactivation of AKT and ERK signaling and prolonged the therapeutic window of trametinib by targeting TICs and thereby preventing the development of acquired resistance in *KRAS*$^{G12/G13}$-mutated LUAD and COAD cells. However, the effectiveness of BI-3406 was lost either in *KRAS*$^{Q61}$-mutated cells or in cells harboring *PIK3CA* co-mutations. For *KRAS*-mutated cells harboring *PIK3CA* co-mutations, constitutive PI3K-AKT signaling bypasses the RTK-dependent PI3K activation that normally occurs due to loss of ERK-dependent negative feedback after trametinib treatment, thereby abrogating the ability of proximal RTK pathway inhibitors including SOS1 to synergizes with trametinib. These data are further consistent with our previous studies showing that SOS2 was required for mutant KRAS-driven transformation, but that transformation could be restored in *Sos2* KO cells by expression of activated PI3K (18).

In *KRAS*$^{Q61}$-mutated cells, the inability of SOS1 inhibitors to synergize with trametinib is likely due to the heterogeneous molecular behavior of codon-specific KRAS mutations with regard to GTP/GDP cycling (77); while G12, G13, and Q61 mutants all show reduced GAP-dependent GTP hydrolysis, Q61 mutants show dramatically reduced intrinsic GTP-hydrolysis compared to G12/G13. The extremely low level of GTP hydrolysis (KRAS inactivation) seen in Q61 mutants makes them much less dependent on RASGEFs for their continued activation compared to G12/G13 mutants (36, 37). Indeed, SHP2 and SOS1 inhibitors enhance the killing effects of MEK inhibitors in *KRAS*$^{G12X}$- and *KRAS*$^{G13X}$-mutated, but not *KRAS*$^{Q61X}$-mutated, tumors (22, 32). Since the ineffectiveness of MEK inhibitors has been attributed not only to feedback RTK-PI3K signaling but also to compensatory ERK reactivation (5, 19, 20), we asked whether

deletion of the RAF/MEK/ERK scaffold KSR1 could cause deep ERK inhibition and enhance the effectiveness of trametinib in *KRAS*-mutated cancer cells that were insensitive to SOS1 inhibition.

We found that in *KRAS*$^{Q61}$/*PIK3CA* mutated LUAD cells, which would be the least sensitive to SOS1 inhibition, *KSR1* KO synergized with trametinib to inhibit ERK signaling, thereby limiting survival and significantly decreasing TIC frequency *in vivo*. Although *PIK3CA* co-mutations are rare in *KRAS*-mutated LUAD, they commonly occur in COAD (78, 79). Thus, we shifted our assessment of *KSR1* KO to COAD cells, where we found *KSR1* KO inhibited the trametinib-induced enrichment of TICs in *KRAS*-mutated COAD cells regardless of *PIK3CA* mutation status. We further showed that these effects were due to KSR1 scaffolding function, as an ERK-binding mutant (KSR1$^{AAAP}$) failed to rescue TIC properties (Aldefluor staining, soft agar growth, clonogenicity) compared to a WT KSR1 transgene.

This finding is consistent with KSR1 function as a RAF/MEK/ERK scaffold and with our previous studies showing KSR1-ERK signaling is essential to mutant *RAS*-driven transformation (38, 40, 80-82). These findings, when coupled to our previous data showing that PI3K/AKT signaling was independent of KSR1 (38, 40) and KSR1 depletion inhibited transformation in *KRAS*/*PIK3CA* co-mutated COAD cells (80-82), give further support to compensatory ERK reactivation as a key component of adaptive resistance to trametinib that can be inhibited by targeting KSR1. Further, the finding that *ksr1*$^{-/-}$ mice are phenotypically normal but resistant to cancer formation (41, 42) highlights the potential of targeting KSR1 to achieve a high therapeutic index. A recently developed KSR inhibitor increased the potency of MEK inhibitors, demonstrating that the use of KSR and MEK inhibitors may be a promising combination therapeutic strategy (44).

In addition to overcoming intrinsic/adaptive resistance, optimal combination therapies would also delay the development of acquired resistance and prolong the window of efficacy for trametinib treatment. Unfortunately, most studies of resistance to RTK/RAS pathway inhibitors including trametinib focus either on synthetic lethality during a short treatment window (0-28 days) (17, 22, 23, 58, 83) or study resistance in a few cell lines established by dose-escalation over several months (84) rather than determining the extent to which combination therapies can delay the onset of acquired resistance. We recently developed an *in situ* resistance assay (ISRA) as a model system to assess acquired resistance to RTK/RAS pathway inhibitors in large cohorts of cell populations (53). Using this assay, we found that SOS1 inhibition prevented the development of trametinib resistance in *KRAS*$^{G12}$-mutated LUAD cells, which represent the majority of *KRAS*-mutated LUADs. Mutations in RTK/RAS pathway members, including KRAS, occur in 75-90% of LUAD, and RTK pathway activation is a major mechanism of acquired resistance in LUADs with *EGFR* mutations (85-94), mutations in alternative RTKs (95-104)), or *KRAS*$^{G12}$ (105-107)) or non-G12C (14-18) mutations likely due to RTK/RAS pathway addiction in these tumors (96, 108-111). In addition to SOS1, the RASGEF SOS2 and the phosphatase/adaptor SHP2 represent proximal RTK signaling intermediates and potential therapeutic targets whose inhibition may limit resistance to RTK/RAS pathway inhibitors in LUAD. In parallel studies, we found that inhibiting proximal RTK signaling by either SHP2 inhibition (53) or *SOS2* deletion (112) delayed or inhibited the development of osimertinib resistance in *EGFR*-mutated LUAD cells. Based on these data, we propose proximal RTK inhibition as a therapeutic strategy to delay resistance to RTK/RAS pathway targeted therapies in a majority of LUADs. However, SOS1 inhibition failed to inhibit resistance in cells with either *KRAS*$^{Q61}$ mutations or with co-occurring *PIK3CA* mutations. In these settings, we found that *KSR1*

KO significantly reduced the number of trametinib resistant colonies suggesting that targeting KSR1 may be a better approach in these genetic backgrounds. While co-occurring *KRAS* and *PIK3CA* mutations are rare in LUAD, ~ 1/3 of *KRAS*-mutated colorectal cancers harbor *PIK3CA* mutations. Thus, we propose that KSR1 may be a better co-therapeutic target compared to SOS1 in COAD.

Our study provides a framework for evaluating and selecting optimal combination therapies to limit both intrinsic/adaptive and acquired resistance to RTK/RAS pathway targeted therapies. Using this framework, we demonstrated that either SOS1 inhibition or KSR1 disruption can increase the efficacy of trametinib and prevent both intrinsic and acquired resistance with genotype-specificity; SOS1 inhibition was more effective in cells harboring $KRAS^{G12/G13}$ mutations with wild-type *PIK3CA*, whereas *KSR1* KO was more effective in $KRAS^{Q61}$-mutated cells and in cells with co-occurring *PIK3CA* mutations. While strategies to inhibit KSR1 are still under development (44, 113), SOS1 inhibitors BI 1701963 [NCT04111458; NCT04975256] and MRTX0902 [NCT05578092] are currently being evaluated in Phase1/2 studies for treatment of *KRAS*-mutated cancers either alone or in combination with trametinib or the $KRAS^{G12C}$ inhibitor adagrasib. Our finding that SOS1 inhibitors delay resistance to trametinib only in $KRAS^{G12/G13}$-mutated cells that lack *PIK3CA* co-mutations has implications for understanding which patient populations will likely benefit from combined SOS1/MEK inhibition and should inform future clinical trial design for SOS1 inhibitor combinations.

**Materials and Methods**

**Cell culture:** Lung and colon cancer cell lines were purchased from ATCC or JCRB (LU99A). After receiving the cells, they were expanded and frozen at passage 3 and 4; cell were passaged once they became 70-80% confluent and maintained in culture for 2-3 months before thawing a new vial as prolonged passaging can alter TIC frequency (114). Cell lines were cultured at 37°C and 5% $CO_2$. Cells were passaged in either RPMI [H727, A549, H358, LU99A, H460] or DMEM [Calu6, H650, H1155, SW620, SW480, LS174T, LoVo, T84, HCT116] supplemented with 10% FBS and 1% penicillin/streptomycin. For signaling experiments, cells were seeded in 24-well micropatterned AggreWell 400 low-attachment plates (StemCell) at $9 \times 10^5$ cells/ well in 2 mL of medium. 24-h post plating, 1 mL of media was replaced with 2× inhibitor. Cells were treated with inhibitor for 0 – 72 hours; for all treatments >24-h, half of the media was removed and replaced with fresh 1× inhibitor daily.

**Production of recombinant lentiviruses and sgRNA studies:** Lentiviruses were produced by co-transfecting MISSION lentiviral packaging mix (Sigma) into 293T cells using Mirus TransIT-Lenti transfection reagent (Mirus Bio # MIR6605) in Opti-MEM (Thermo Scientific #31-985-062). 48-h post-transfection, viral supernatants were collected and filtered. Viral supernatants were then either stored at -80°C or used immediately to infect cells in combination with polybrene at 8 μg/mL.

**Generation of pooled genomic *SOS1* KO cell lines**: For *SOS1* KO studies, cells were infected with lentiviruses based on pLentiCRISPRv2 with either a non-targeting sgRNA (NT) or a sgRNA targeting SOS1 (70). 48-h post-infection, cells were selected in 4 μg/mL Puromycin (Invitrogen). 7-10 days after selection, cells were analyzed for SOS1

or KSR1 expression. Cell populations showing >80% deletion were used for further study.

**Generation of clonal genomic *KSR1* KO cell lines**: sgRNA sequences targeting KSR1 or non-targeting control were inserted into pCAG-SpCas9-GFP-U6-gRNA (Addgene #79144, gift of Jizhong Zou). PEI transfection was used to insert pCAG-SpCas9-GFP-U6-sgKSR1 or non-targeting control into H460 and HCT116 cells. GFP-selection by fluorescence-activated cell sorting was performed 48-h post-transfection, and colonies were grown out with the use of cloning rings.

**Generation of pooled genomic *KSR1* KO cell lines**: sgRNA sequences targeting KSR1 or non-targeting control were inserted into pLentiCRISPRv2GFP (Addgene #82416). The constructs were PEI transfected into HEK293T cells along with psPAX2 lentiviral packaging construct (Addgene #12259) and pMD2.G envelope construct (Addgene #12259). Lentivirus-containing media was harvested at 96-h, and added to SW480, LoVo, LS174T, and T84 cells. GFP+ cells were selected by fluorescence-activated cell sorting.

**Generation of KSR1 addback in clonal genomic *KSR1* KO cell lines**: Murine KSR1 was cloned into MSCV-IRES-KSR1-GFP (Addgene #25973) and PEI transfected into HEK293T cells along with pUMVC retroviral packaging construct (Addgene # 8449) and VSVG envelope construct (Addgene #8454). Lentivirus-containing media was harvested at 96-h and added to clonal *KSR1* KO HCT116 and H460 cells. GFP-selection was performed by fluorescence-activated cell sorting 48-h post-transfection.

**Single Cell Colony-forming Assay:** Cells were DAPI-stained for viability determination and live cells were single cell sorted as one cell per well into a 96-well, U-bottom, non-adherent plate (Takara Bio). Cells were grown for 14 days, after which colony formation was determined using CellTiter Glo® viability assay (Promega) performed according to manufacturer instructions.

**Flow cytometry:** Cells were plated in 10 or 6 cm tissue-culture treated plates and allowed to adhere for 24-48-h prior to drug treatment. Once cells were 50-75% confluent, cells were treated with the indicated concentration of trametinib or selumetinib for 72-h. After the 72-h treatment, cells were harvested by trypsinization, spun down, resuspended in Aldefluor Assay Buffer (StemCell) at $1 \times 10^6$ cells/mL, and stained for ALDH activity using the Aldefluor Assay Kit per manufacturer's instructions. An aliquot of cells was pre-treated with the ALDH inhibitor DEAB, which inhibits ALDH enzymatic activity and is thus used as a negative gating control. Data were analyzed using FloJo with and are presented as the % of cells showing ALDH activity over DEAB controls.

**Soft Agar Colony-forming Assay:** $1 \times 10^3$ cells per dish were plated onto 35mm dishes in 0.4% NuSieve Agarose (Lonza #50081). Six replicates of each condition were plated. At 14 days, colony formation was assessed by counting colonies > 100 μM in their largest diameter.

**Cell lysis and Western blotting:** Cells were lysed in RIPA buffer (1% NP-40, 0.1% SDS, 0.1% Na-deoxycholate, 10% glycerol, 0.137 M NaCl, 20 mM Tris pH [8.0], protease (Biotool #B14002) and phosphatase (Biotool #B15002) inhibitor cocktails) for 20 min at 4°C and spun at 10,000 RPM for 10 min. Clarified lysates were boiled in SDS

sample buffer containing 100 mM DTT for 10 min prior to western blotting. Proteins were resolved by sodium dodecyl sulfate-polyacrylamide (Criterion TGX precast) gel electrophoresis and transferred to nitrocellulose membranes. Western blots were developed by multiplex Western blotting using anti-SOS1 (Santa Cruz sc-256; 1:500), anti-β-actin (Sigma AC-15; 1:5,000 or Santa Cruz Biotechnology sc-47778, 1:2000 dilution), anti-α-tubulin (Abcam ab89984 1:2000); anti-pERK1/2 (Cell Signaling 4370; 1:1,000), anti-ERK1/2 (Cell Signaling 4696; 1:1000), anti-pAKT Ser473 (Cell Signaling 4060; 1:1000), anti-AKT (Cell Signaling 2920; 1:1000), anti-KSR1 (Abcam ab68483, 1:750 dilution), primary antibodies. Anti-mouse, anti-rabbit, and anti-chicken secondary antibodies conjugated to IRDye680 or IRDye800 (LI-COR; 1:20,000) were used to probe primary antibodies. Western blot protein bands were detected and quantified using the Odyssey system (LI-COR).

**Extreme Limiting Dilution Assays (ELDA):** *In vivo:* In equal volumes of 50% Cultrex® Basement Membrane Extract (R&D Systems) 50% Dulbecco's Modified Eagle Medium (Cytiva), dilutions ranging from 5 to 1000 cells were injected subcutaneously into the shoulder and hip of 6-8-week-old triple immunodeficient male NOD-Prkdc$^{em26Cd52}$Il2rg$^{em26Cd22}$/NjuCr (NCG, Charles River) mice. Mice were monitored for tumor formation by palpation. Once tumor size reached 1cm$^3$, mice were sacrificed and tumors were excised. TIC frequency and significance between groups was calculated by ELDA website https://bioinf.wehi.edu.au/software/elda/ (73).

*In situ:* Cells were seeded in 96-well ultra-low attachment flat bottomed plates (Corning Corstar #3474) at decreasing cell concentrations (1000 cells/well – 1 cell/well) at half log intervals (1000, 300, 100, 30, 10, 3, 1), 12 wells per condition with the exception of the 10 cells/well condition, for which 24 wells were seeded. Cells were cultured for 7-10

days, and wells with spheroids > 100 mM were scored as spheroid positive. TIC frequency and significance between groups was calculated by ELDA website https://bioinf.wehi.edu.au/software/elda/ (73). To assess the effect of trametinib on TIC frequency, cells were left untreated or were pre-treated with the indicated dose of trametinib or selumetinib for 72-h, after which cells were rested for 48-72-h prior to plating. To assess the effect of SOS1 inhibition, cells were seeded ± 300 nM BI-3406.

**Bliss Independence Analysis for Synergy:** Cells were seeded at 750 cells per well in 100 mL in the inner-60 wells of 96-well ultra-low attachment round bottomed plates (Corning #7007) or Nunc NucleonSphera microplates (ThermoFisher # 174929) and allowed to coalesce as spheroids for 24-48 hr prior to drug treatment. Cells were treated with drug for 96-h prior to assessment of cell viability using CellTiter Glo® 2.0 (Promega). For all studies, outer wells (rows A and H, columns 1 and 12) were filled with 200 mL of PBS to buffer inner cells from temperature and humidity fluctuations. Triplicate wells of cells were then treated with increasing concentrations trametinib alone, BI-3406 alone, or the combination of trametinib + BI-3406 in a 9 × 9 matrix of drug combinations on a similog scale for 72-h (adherent cultures) or 96-h (spheroids). Cell viability was assessed using CellTiter Glo® 2.0 (30 mL/well). Luminescence was assessed using a Bio-Tek Cytation five multi-mode plate reader. Data were normalized to the maximum luminescence reading of untreated cells, and individual drug $EC_{50}$ values were calculated using Prism9 by non-linear regression using log(inhibitor) vs. response. For all drug-treatment studies, the untreated sample for each cell line was set to 100%. This would mask any differences in 3D cell proliferation seen between cell lines. Excess over Bliss was calculated as the Actual Effect – Expected Effect as

outlined in (70). The SUM EOB is calculated by taking the sum of excess over bliss values across the 9 × 9 treatment matrix. EOB values > 0 indicate increasing synergy.

**Resistance Assays:** Cells were plated at low density (250 cells/well) in replicate 96-well plates, and each plate was treated with the indicated doses of trametinib ± BI-3406. Wells were fed and assessed weekly for outgrowth, wells that were > 50% confluent were scored as resistant to the given dose of trametinib. Data are plotted as a Kaplan-Meier survival curve; significance was assessed by comparing Kaplan-Meyer Meier curves using Prism 9.

**List of Key Resources:**

KSR1 antibody: Abcam ab68483, 1:750 dilution

β-actin antibody: Santa Cruz Biotechnology sc-47778, 1:2000 dilution

β-actin antibody: Sigma AC-15; 1:5,000 dilution

SOS1 antibody: Santa Cruz sc-256; 1:500 dilution

a-tubulin antibody: Abcam ab89984 1:2000 dilution

pERK1/2 antibody: Cell Signaling 4370; 1:1,000 dilution

ERK1/2 antibody: Cell Signaling 4696; 1:1000 dilution

pAKT Ser473 antibody: (Cell Signaling 4060; 1:1000 dilution

AKT antibody: Cell Signaling 2920; 1:1000 dilution

KSR1 sgRNA sequences:

CR1 5' TTGGATGCGCGGCGGGAAAG 3'

CR2 5' CTGACACGGAGATGGAGCGT 3'

NT sgRNA sequence: 5' CCATATCGGGGCGAGACATG 3'

SOS1 sgRNA sequence: 5' GCATCCTTTCCAGTGTACTC 3'

Plasmid catalog numbers listed in the sections above.

**Acknowledgments**

We thank the UNMC Cell Analysis Facility and UNMC Animal Facility. **Funding**: This work was supported by funding from the NIH (R01 CA255232 and R21 CA267515 to R.L.K and P20 GM121316 to R.E.L), the CDMRP Lung Cancer Research Program (LC180213 to R.L.K. and LC210123 to R.E.L and R.L.K.), Nebraska Department of Health and Human Services (LB506 and LB606 awards to R.E.L.) and a CRADA from Boehringer Ingelheim (to R.L.K). H.M.V. is supported by funding from NIH T32CA009476. The funders had no role in the study design, data collection and interpretation, or the decision to submit the work for publication. The opinions and assertions expressed herein are those of the authors and are not to be construed as reflecting the views of Uniformed Services University of the Health Sciences or the United States Department of Defense. **Competing interests:** The Kortum laboratory receives funding from Boehringer Ingelheim to study SOS1 as a therapeutic target in *RAS*-mutated cancers.

## References


1. A. D. Cox, S. W. Fesik, A. C. Kimmelman, J. Luo, C. J. Der, Drugging the undruggable RAS: Mission Possible? *Nature Reviews Drug Discovery* **13**, 828-851 (2014).

2. I. A. Prior, F. E. Hood, J. L. Hartley, The Frequency of Ras Mutations in Cancer. *Cancer Res* **80**, 2969-2974 (2020).

3. M. Reck, D. P. Carbone, M. Garassino, F. Barlesi, Targeting KRAS in non-small-cell lung cancer: recent progress and new approaches. *Annals of Oncology* **32**, 1101-1110 (2021).

4. A. S. Bear *et al.*, Biochemical and functional characterization of mutant KRAS epitopes validates this oncoprotein for immunological targeting. *Nature Communications* **12** (2021).

5. T. K. Hayes *et al.*, Long-Term ERK Inhibition in KRAS-Mutant Pancreatic Cancer Is Associated with MYC Degradation and Senescence-like Growth Suppression. *Cancer Cell* **29**, 75-89 (2016).

6. A. M. Waters, C. J. Der, KRAS: The Critical Driver and Therapeutic Target for Pancreatic Cancer. *Cold Spring Harb Perspect Med* **8** (2018).

7. I. Ozkan-Dagliyan *et al.*, Low-Dose Vertical Inhibition of the RAF-MEK-ERK Cascade Causes Apoptotic Death of KRAS Mutant Cancers. *Cell Rep* **31**, 107764 (2020).

8. M. V. Huynh *et al.*, Functional and biological heterogeneity of KRAS(Q61) mutations. *Sci Signal* **15**, eabn2694 (2022).

9. E. M. Terrell *et al.*, Distinct Binding Preferences between Ras and Raf Family Members and the Impact on Oncogenic Ras Signaling. *Mol Cell* **76**, 872-884 e875 (2019).

10. J. N. Diehl *et al.*, Targeting the ERK mitogen-activated protein kinase cascade for the treatment of KRAS-mutant pancreatic cancer. *Adv Cancer Res* **153**, 101-130 (2022).

11. K. K. Ciombor, T. Bekaii-Saab, Selumetinib for the treatment of cancer. *Expert Opin Investig Drugs* **24**, 111-123 (2015).

12. C. J. M. Wright, P. L. McCormack, Trametinib: First Global Approval. *Drugs* **73**, 1245-1254 (2013).

13. C. Delahaye *et al.*, Early Steps of Resistance to Targeted Therapies in Non-Small-Cell Lung Cancer. *Cancers (Basel)* **14** (2022).

14. A. B. Turke *et al.*, MEK inhibition leads to PI3K/AKT activation by relieving a negative feedback on ERBB receptors. *Cancer Res* **72**, 3228-3237 (2012).

15. P. Pettazzoni *et al.*, Genetic events that limit the efficacy of MEK and RTK inhibitor therapies in a mouse model of KRAS-driven pancreatic cancer. *Cancer Res* **75**, 1091-1101 (2015).

16. M. L. Sos *et al.*, Identifying genotype-dependent efficacy of single and combined PI3K- and MAPK-pathway inhibition in cancer. *Proc Natl Acad Sci U S A* **106**, 18351-18356 (2009).

17. E. Manchado *et al.*, A combinatorial strategy for treating KRAS-mutant lung cancer. *Nature* **534**, 647-651 (2016).

18. E. Sheffels *et al.*, Oncogenic RAS isoforms show a hierarchical requirement for the guanine nucleotide exchange factor SOS2 to mediate cell transformation. *Sci Signal* **11** (2018).

19. A. A. Samatar, P. I. Poulikakos, Targeting RAS-ERK signalling in cancer: promises and challenges. *Nat Rev Drug Discov* **13**, 928-942 (2014).

20. A. Hong *et al.*, Durable Suppression of Acquired MEK Inhibitor Resistance in Cancer by Sequestering MEK from ERK and Promoting Antitumor T-cell Immunity. *Cancer Discov* **11**, 714-735 (2021).

21. H. F. Cabanos, A. N. Hata, Emerging Insights into Targeted Therapy-Tolerant Persister Cells in Cancer. *Cancers (Basel)* **13** (2021).

22. C. Fedele *et al.*, SHP2 Inhibition Prevents Adaptive Resistance to MEK Inhibitors in Multiple Cancer Models. *Cancer Discov* **8**, 1237-1249 (2018).

23. O. Kauko *et al.*, PP2A inhibition is a druggable MEK inhibitor resistance mechanism in KRAS-mutant lung cancer cells. *Sci Transl Med* **10** (2018).

24. E. Batlle, H. Clevers, Cancer stem cells revisited. *Nature Medicine* **23**, 1124-1134 (2017).

25. T. Shibue, R. A. Weinberg, EMT, CSCs, and drug resistance: the mechanistic link and clinical implications. *Nat Rev Clin Oncol* **14**, 611-629 (2017).

26. A. Wang, L. Qu, L. Wang, At the crossroads of cancer stem cells and targeted therapy resistance. *Cancer Lett* **385**, 87-96 (2017).

27. T. Zhan *et al.*, MEK inhibitors activate Wnt signalling and induce stem cell plasticity in colorectal cancer. *Nature Communications* **10**, 2197 (2019).

28. T. Shi *et al.*, Conservation of protein abundance patterns reveals the regulatory architecture of the EGFR-MAPK pathway. *Sci Signal* **9**, rs6 (2016).

29. C. R. Evelyn *et al.*, Rational design of small molecule inhibitors targeting the Ras GEF, SOS1. *Chem Biol* **21**, 1618-1628 (2014).

30. C. R. Evelyn *et al.*, Combined rational design and a high throughput screening platform for identifying chemical inhibitors of a Ras-activating enzyme. *J Biol Chem* **290**, 12879-12898 (2015).

31. R. C. Hillig *et al.*, Discovery of potent SOS1 inhibitors that block RAS activation via disruption of the RAS-SOS1 interaction. *Proc Natl Acad Sci U S A* **116**, 2551-2560 (2019).

32. M. H. Hofmann *et al.*, BI-3406, a Potent and Selective SOS1-KRAS Interaction Inhibitor, Is Effective in KRAS-Driven Cancers through Combined MEK Inhibition. *Cancer Discov* **11**, 142-157 (2021).

33. D. Kessler, D. Gerlach, N. Kraut, D. B. McConnell, Targeting Son of Sevenless 1: The pacemaker of KRAS. *Curr Opin Chem Biol* **62**, 109-118 (2021).

34. J. Ramharter *et al.*, One Atom Makes All the Difference: Getting a Foot in the Door between SOS1 and KRAS. *J Med Chem* **64**, 6569-6580 (2021).

35. R. C. Hillig, B. Bader, Targeting RAS oncogenesis with SOS1 inhibitors. *Adv Cancer Res* **153**, 169-203 (2022).

36. J. C. Hunter *et al.*, Biochemical and Structural Analysis of Common Cancer-Associated KRAS Mutations. *Mol Cancer Res* **13**, 1325-1335 (2015).

37. M. J. Smith, B. G. Neel, M. Ikura, NMR-based functional profiling of RASopathies and oncogenic RAS mutations. *Proc Natl Acad Sci U S A* **110**, 4574-4579 (2013).

38. R. L. Kortum, R. E. Lewis, The molecular scaffold KSR1 regulates the proliferative and oncogenic potential of cells. *Mol Cell Biol* **24**, 4407-4416 (2004).

39. R. L. Kortum *et al.*, The molecular scaffold kinase suppressor of Ras 1 (KSR1) regulates adipogenesis. *Mol Cell Biol* **25**, 7592-7604 (2005).

40. R. L. Kortum *et al.*, The molecular scaffold kinase suppressor of Ras 1 is a modifier of RasV12-induced and replicative senescence. *Mol Cell Biol* **26**, 2202-2214 (2006).

41. J. Lozano *et al.*, Deficiency of Kinase Suppressor of Ras1 Prevents Oncogenic Ras Signaling in Mice. *Cancer Research* **63**, 4232-4238 (2003).

42. A. Nguyen *et al.*, Kinase suppressor of Ras (KSR) is a scaffold which facilitates mitogen-activated protein kinase activation in vivo. *Mol Cell Biol* **22**, 3035-3045 (2002).

43. G. Paniagua *et al.*, KSR induces RAS-independent MAPK pathway activation and modulates the efficacy of KRAS inhibitors. *Mol Oncol* **16**, 3066-3081 (2022).

44. N. S. Dhawan, A. P. Scopton, A. C. Dar, Small molecule stabilization of the KSR inactive state antagonizes oncogenic Ras signalling. *Nature* **537**, 112-116 (2016).

45. T. A. Ahmed *et al.*, SHP2 Drives Adaptive Resistance to ERK Signaling Inhibition in Molecularly Defined Subsets of ERK-Dependent Tumors. *Cell Rep* **26**, 65-78 e65 (2019).

46. J. Codony-Servat *et al.*, Cancer Stem Cell Biomarkers in EGFR-Mutation-Positive Non-Small-Cell Lung Cancer. *Clin Lung Cancer* **20**, 167-177 (2019).

47. C. Shao *et al.*, Essential role of aldehyde dehydrogenase 1A3 for the maintenance of non-small cell lung cancer stem cells is associated with the STAT3 pathway. *Clin Cancer Res* **20**, 4154-4166 (2014).

48. S. Hu *et al.*, Antagonism of EGFR and Notch limits resistance to EGFR inhibitors and radiation by decreasing tumor-initiating cell frequency. *Sci Transl Med* **9** (2017).

49. J. P. Sullivan *et al.*, Aldehyde dehydrogenase activity selects for lung adenocarcinoma stem cells dependent on notch signaling. *Cancer Res* **70**, 9937-9948 (2010).

50. G. L. Gonzalez-Del Pino *et al.*, Allosteric MEK inhibitors act on BRAF/MEK complexes to block MEK activation. *Proc National Acad Sci* **118**, e2107207118 (2021).

51. M. Cacace Angela *et al.*, Identification of Constitutive and Ras-Inducible Phosphorylation Sites of KSR: Implications for 14-3-3 Binding, Mitogen-Activated Protein Kinase Binding, and KSR Overexpression. *Molecular and Cellular Biology* **19**, 229-240 (1999).

52. M. M. McKay, D. A. Ritt, D. K. Morrison, Signaling dynamics of the KSR1 scaffold complex. *Proc Natl Acad Sci U S A* **106**, 11022-11027 (2009).

53. N. E. Sealover *et al.*, In situ modeling of acquired resistance to RTK/RAS pathway targeted therapies. *bioRxiv* 10.1101/2023.01.27.525958, 2023.2001.2027.525958 (2023).

54. J. K. Voice, R. L. Klemke, A. Le, J. H. Jackson, Four human ras homologs differ in their abilities to activate Raf-1, induce transformation, and stimulate cell motility. *J Biol Chem* **274**, 17164-17170 (1999).

55. J. Yan, S. Roy, A. Apolloni, A. Lane, J. F. Hancock, Ras isoforms vary in their ability to activate Raf-1 and phosphoinositide 3-kinase. *J Biol Chem* **273**, 24052-24056 (1998).

56. M. Hamilton, A. Wolfman, Oncogenic Ha-Ras-dependent mitogen-activated protein kinase activity requires signaling through the epidermal growth factor receptor. *J Biol Chem* **273**, 28155-28162 (1998).

57. E. Sheffels, N. E. Sealover, P. L. Theard, R. L. Kortum, Anchorage-independent growth conditions reveal a differential SOS2 dependence for transformation and survival in RAS-mutant cancer cells. *Small GTPases* **12**, 67-78 (2021).

58. R. Sulahian *et al.*, Synthetic Lethal Interaction of SHOC2 Depletion with MEK Inhibition in RAS-Driven Cancers. *Cell Rep* **29**, 118-134 e118 (2019).

59. G. R. Anderson *et al.*, A Landscape of Therapeutic Cooperativity in KRAS Mutant Cancers Reveals Principles for Controlling Tumor Evolution. *Cell Rep* **20**, 999-1015 (2017).

60. C. Scholl *et al.*, Synthetic lethal interaction between oncogenic KRAS dependency and STK33 suppression in human cancer cells. *Cell* **137**, 821-834 (2009).

61. A. Singh *et al.*, A gene expression signature associated with "K-Ras addiction" reveals regulators of EMT and tumor cell survival. *Cancer Cell* **15**, 489-500 (2009).

62. A. Singh *et al.*, TAK1 inhibition promotes apoptosis in KRAS-dependent colon cancers. *Cell* **148**, 639-650 (2012).

63. O. A. Balbin *et al.*, Reconstructing targetable pathways in lung cancer by integrating diverse omics data. *Nat Commun* **4**, 2617 (2013).

64. S. Lamba *et al.*, RAF suppression synergizes with MEK inhibition in KRAS mutant cancer cells. *Cell Rep* **8**, 1475-1483 (2014).

65. Z. Zhang, G. Jiang, F. Yang, J. Wang, Knockdown of mutant K-ras expression by adenovirus-mediated siRNA inhibits the in vitro and in vivo growth of lung cancer cells. *Cancer Biol Ther* **5**, 1481-1486 (2006).

66. S. Fujita-Sato *et al.*, Enhanced MET Translation and Signaling Sustains K-Ras-Driven Proliferation under Anchorage-Independent Growth Conditions. *Cancer Res* **75**, 2851-2862 (2015).

67. F. McCormick, KRAS as a Therapeutic Target. *Clin Cancer Res* **21**, 1797-1801 (2015).

68. A. Rotem *et al.*, Alternative to the soft-agar assay that permits high-throughput drug and genetic screens for cellular transformation. *Proc Natl Acad Sci U S A* **112**, 5708-5713 (2015).

69. M. R. Janes *et al.*, Targeting KRAS Mutant Cancers with a Covalent G12C-Specific Inhibitor. *Cell* **172**, 578-589 e517 (2018).

70. P. L. Theard *et al.*, Marked synergy by vertical inhibition of EGFR signaling in NSCLC spheroids shows SOS1 is a therapeutic target in EGFR-mutated cancer. *Elife* **9** (2020).

71. S. Mainardi *et al.*, SHP2 is required for growth of KRAS-mutant non-small-cell lung cancer in vivo. *Nat Med* **24**, 961-967 (2018).

72. R. J. Nichols *et al.*, RAS nucleotide cycling underlies the SHP2 phosphatase dependence of mutant BRAF-, NF1- and RAS-driven cancers. *Nat Cell Biol* **20**, 1064-1073 (2018).

73. Y. Hu, G. K. Smyth, ELDA: extreme limiting dilution analysis for comparing depleted and enriched populations in stem cell and other assays. *J Immunol Methods* **347**, 70-78 (2009).

74. S. Misale *et al.*, Vertical suppression of the EGFR pathway prevents onset of resistance in colorectal cancers. *Nat Commun* **6**, 8305 (2015).

75. E. M. Tricker *et al.*, Combined EGFR/MEK Inhibition Prevents the Emergence of Resistance in EGFR-Mutant Lung Cancer. *Cancer Discov* **5**, 960-971 (2015).

76. K. J. Kurppa *et al.*, Treatment-Induced Tumor Dormancy through YAP-Mediated Transcriptional Reprogramming of the Apoptotic Pathway. *Cancer Cell* **37**, 104-122 e112 (2020).

77. N. E. Sealover, R. L. Kortum, Heterogeneity in RAS mutations: One size does not fit all. *Sci Signal* **15**, eadc9816 (2022).

78. E. Cerami *et al.*, The cBio cancer genomics portal: an open platform for exploring multidimensional cancer genomics data. *Cancer Discov* **2**, 401-404 (2012).

79. J. Gao *et al.*, Integrative analysis of complex cancer genomics and clinical profiles using the cBioPortal. *Sci Signal* **6**, pl1 (2013).

80. K. W. Fisher *et al.*, AMPK Promotes Aberrant PGC1beta Expression To Support Human Colon Tumor Cell Survival. *Mol Cell Biol* **35**, 3866-3879 (2015).

81. J. L. McCall *et al.*, KSR1 and EPHB4 Regulate Myc and PGC1β To Promote Survival of Human Colon Tumors. *Mol Cell Biol* **36**, 2246-2261 (2016).

82. C. Rao *et al.*, KSR1-and ERK-dependent translational regulation of the epithelial-to-mesenchymal transition. *Elife* **10** (2021).

83. C. Sun *et al.*, Intrinsic resistance to MEK inhibition in KRAS mutant lung and colon cancer through transcriptional induction of ERBB3. *Cell Rep* **7**, 86-93 (2014).

84. D. A. Farnsworth *et al.*, MEK inhibitor resistance in lung adenocarcinoma is associated with addiction to sustained ERK suppression. *NPJ Precis Oncol* **6**, 88 (2022).

85. C. A. Eberlein *et al.*, Acquired Resistance to the Mutant-Selective EGFR Inhibitor AZD9291 Is Associated with Increased Dependence on RAS Signaling in Preclinical Models. *Cancer Res* **75**, 2489-2500 (2015).

86. P. Shi *et al.*, Met gene amplification and protein hyperactivation is a mechanism of resistance to both first and third generation EGFR inhibitors in lung cancer treatment. *Cancer Lett* **380**, 494-504 (2016).

87. S. La Monica *et al.*, Trastuzumab emtansine delays and overcomes resistance to the third-generation EGFR-TKI osimertinib in NSCLC EGFR mutated cell lines. *J Exp Clin Cancer Res* **36**, 174 (2017).

88. M. Mancini *et al.*, An oligoclonal antibody durably overcomes resistance of lung cancer to third-generation EGFR inhibitors. *EMBO Mol Med* **10**, 294-308 (2018).

89. D. Romaniello *et al.*, A Combination of Approved Antibodies Overcomes Resistance of Lung Cancer to Osimertinib by Blocking Bypass Pathways. *Clin Cancer Res* **24**, 5610-5621 (2018).

90. J. H. Park *et al.*, Activation of the IGF1R pathway potentially mediates acquired resistance to mutant-selective 3rd-generation EGF receptor tyrosine kinase inhibitors in advanced non-small cell lung cancer. *Oncotarget* **7**, 22005-22015 (2016).

91. D. Kim *et al.*, AXL degradation in combination with EGFR-TKI can delay and overcome acquired resistance in human non-small cell lung cancer cells. *Cell Death Dis* **10**, 361 (2019).

92. H. Taniguchi *et al.*, AXL confers intrinsic resistance to osimertinib and advances the emergence of tolerant cells. *Nat Commun* **10**, 259 (2019).

93. K. Namba *et al.*, Activation of AXL as a Preclinical Acquired Resistance Mechanism Against Osimertinib Treatment in EGFR-Mutant Non-Small Cell Lung Cancer Cells. *Mol Cancer Res* **17**, 499-507 (2019).

94. T. Jimbo *et al.*, DS-1205b, a novel selective inhibitor of AXL kinase, blocks resistance to EGFR-tyrosine kinase inhibitors in a non-small cell lung cancer xenograft model. *Oncotarget* **10**, 5152-5167 (2019).

95. Y. Pan, C. Deng, Z. Qiu, C. Cao, F. Wu, The Resistance Mechanisms and Treatment Strategies for ALK-Rearranged Non-Small Cell Lung Cancer. *Front Oncol* **11**, 713530 (2021).

96. M. G. Ferrara *et al.*, Oncogene-Addicted Non-Small-Cell Lung Cancer: Treatment Opportunities and Future Perspectives. *Cancers (Basel)* **12** (2020).

97. G. Hrustanovic *et al.*, RAS-MAPK dependence underlies a rational polytherapy strategy in EML4-ALK-positive lung cancer. *Nat Med* **21**, 1038-1047 (2015).

98. A. Vaishnavi *et al.*, Inhibition of MEK1/2 Forestalls the Onset of Acquired Resistance to Entrectinib in Multiple Models of NTRK1-Driven Cancer. *Cell Rep* **32**, 107994 (2020).

99. B. M. Ku *et al.*, Entrectinib resistance mechanisms in ROS1-rearranged non-small cell lung cancer. *Invest New Drugs* **38**, 360-368 (2020).

100. K. D. Davies *et al.*, Resistance to ROS1 inhibition mediated by EGFR pathway activation in non-small cell lung cancer. *PLoS One* **8**, e82236 (2013).

101. S. K. Nelson-Taylor *et al.*, Resistance to RET-Inhibition in RET-Rearranged NSCLC Is Mediated By Reactivation of RAS/MAPK Signaling. *Mol Cancer Ther* **16**, 1623-1633 (2017).

102. S. Kim *et al.*, Acquired Resistance of MET-Amplified Non-small Cell Lung Cancer Cells to the MET Inhibitor Capmatinib. *Cancer Res Treat* **51**, 951-962 (2019).

103. T. Takeda *et al.*, YES1 activation induces acquired resistance to neratinib in HER2-amplified breast and lung cancers. *Cancer Sci* **111**, 849-856 (2020).

104. H. Torigoe *et al.*, Therapeutic strategies for afatinib-resistant lung cancer harboring HER2 alterations. *Cancer Sci* **109**, 1493-1502 (2018).

105. J. Hallin *et al.*, The KRAS(G12C) Inhibitor MRTX849 Provides Insight toward Therapeutic Susceptibility of KRAS-Mutant Cancers in Mouse Models and Patients. *Cancer Discov* **10**, 54-71 (2020).

106. M. B. Ryan *et al.*, Vertical Pathway Inhibition Overcomes Adaptive Feedback Resistance to KRAS(G12C) Inhibition. *Clin Cancer Res* **26**, 1633-1643 (2020).

107. J. Y. Xue *et al.*, Rapid non-uniform adaptation to conformation-specific KRAS(G12C) inhibition. *Nature* **577**, 421-425 (2020).

108. J. Rotow, T. G. Bivona, Understanding and targeting resistance mechanisms in NSCLC. *Nat Rev Cancer* **17**, 637-658 (2017).

109. R. C. Doebele, Acquired Resistance Is Oncogene and Drug Agnostic. *Cancer Cell* **36**, 347-349 (2019).

110. A. Vaishnavi *et al.*, EGFR Mediates Responses to Small-Molecule Drugs Targeting Oncogenic Fusion Kinases. *Cancer Res* **77**, 3551-3563 (2017).

111. E. Sheffels, R. L. Kortum, Breaking Oncogene Addiction: Getting RTK/RAS-Mutated Cancers off the SOS. *J Med Chem* **64**, 6566-6568 (2021).

112. P. L. Theard *et al.*, SOS2 regulates the threshold of mutant EGFR-dependent oncogenesis. *bioRxiv* 10.1101/2023.01.20.524989, 2023.2001.2020.524989 (2023).

113. Z. M. Khan *et al.*, Structural basis for the action of the drug trametinib at KSR-bound MEK. *Nature* **588**, 509-514 (2020).

114. K. Qureshi-Baig, P. Ullmann, S. Haan, E. Letellier, Tumor-Initiating Cells: a criTICal review of isolation approaches and new challenges in targeting strategies. *Molecular Cancer* **16** (2017).

**Figures and Tables**

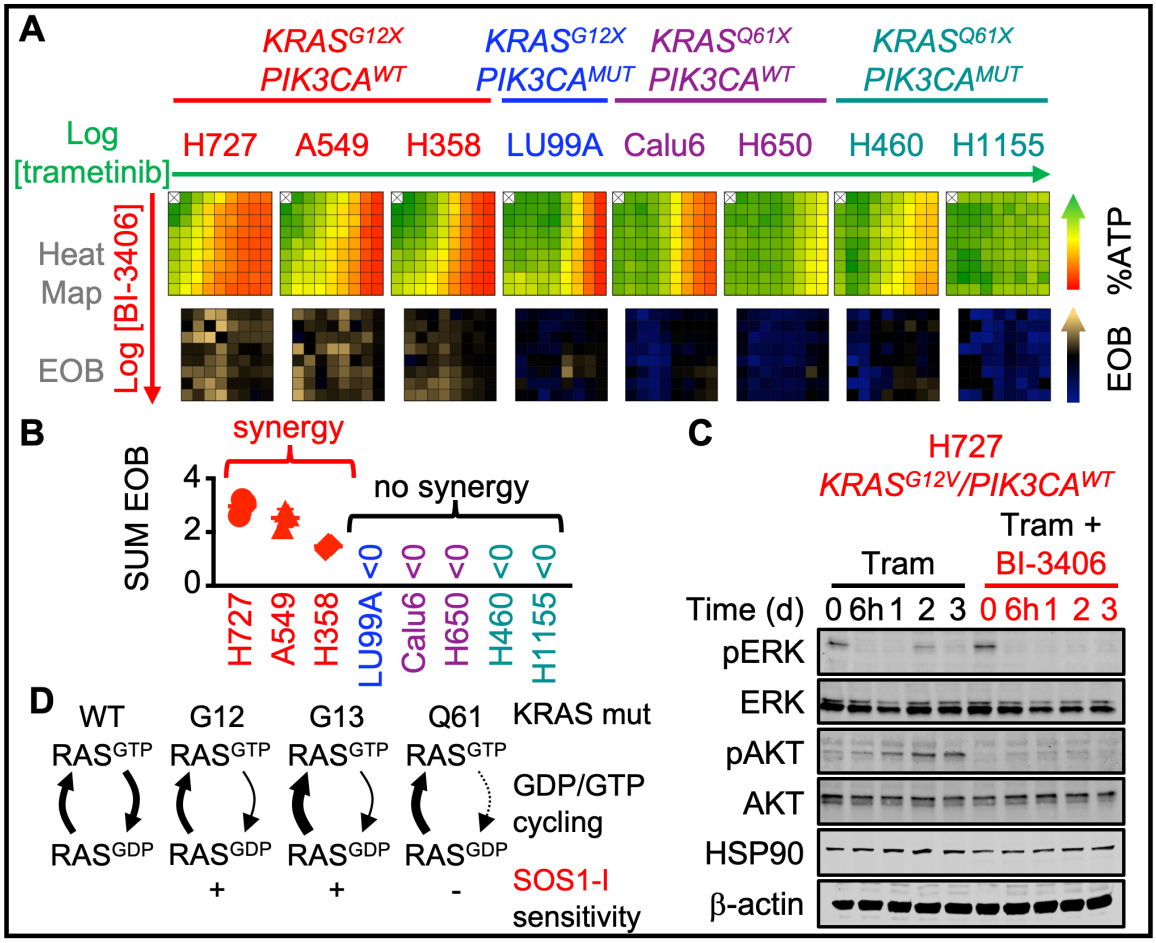


**Figure 1.** MEK and SOS1 inhibition synergize to prevent rebound signaling in *KRAS*$^{G12}$/*PIK3CA*$^{WT}$-mutated LUAD cells.

**(A)** Heat map of cell viability (top) and excess over Bliss (EOB, bottom) for the indicated *KRAS*-mutated LUAD cell lines treated with increasing (semi-log) doses of trametinib ($10^{-10.5}$ – $10^{-7}$), BI-3406 ($10^{-9}$ – $10^{-5.5}$) or the combination of trametinib + BI-3406 under 3D spheroid culture conditions. The *KRAS* and *PIK3CA* mutational status of each cell line is indicated. Data are the mean from three independent experiments, each experiment had three technical replicates. **(B)** The sum of EOB for the 9×9 matrix of trametinib + BI3406 treatments from **A**. EOB > 0 indicates increasing synergy. Data are presented as mean ± s.d. from *N*=3 independent experiments. **(C)** Western blots of WCLs of 3D spheroid cultured H727 cells treated with trametinib (10 nM) ± BI-3406 (300 nM) for the indicated times. Western blots for pERK, ERK, pAKT (Ser 473), AKT, HSP90, and β-actin are representative from three independent experiments. **(D)** Relative efficiencies of RAS GTP/GDP cycling for different oncogenic RAS mutants compared to WT RAS.

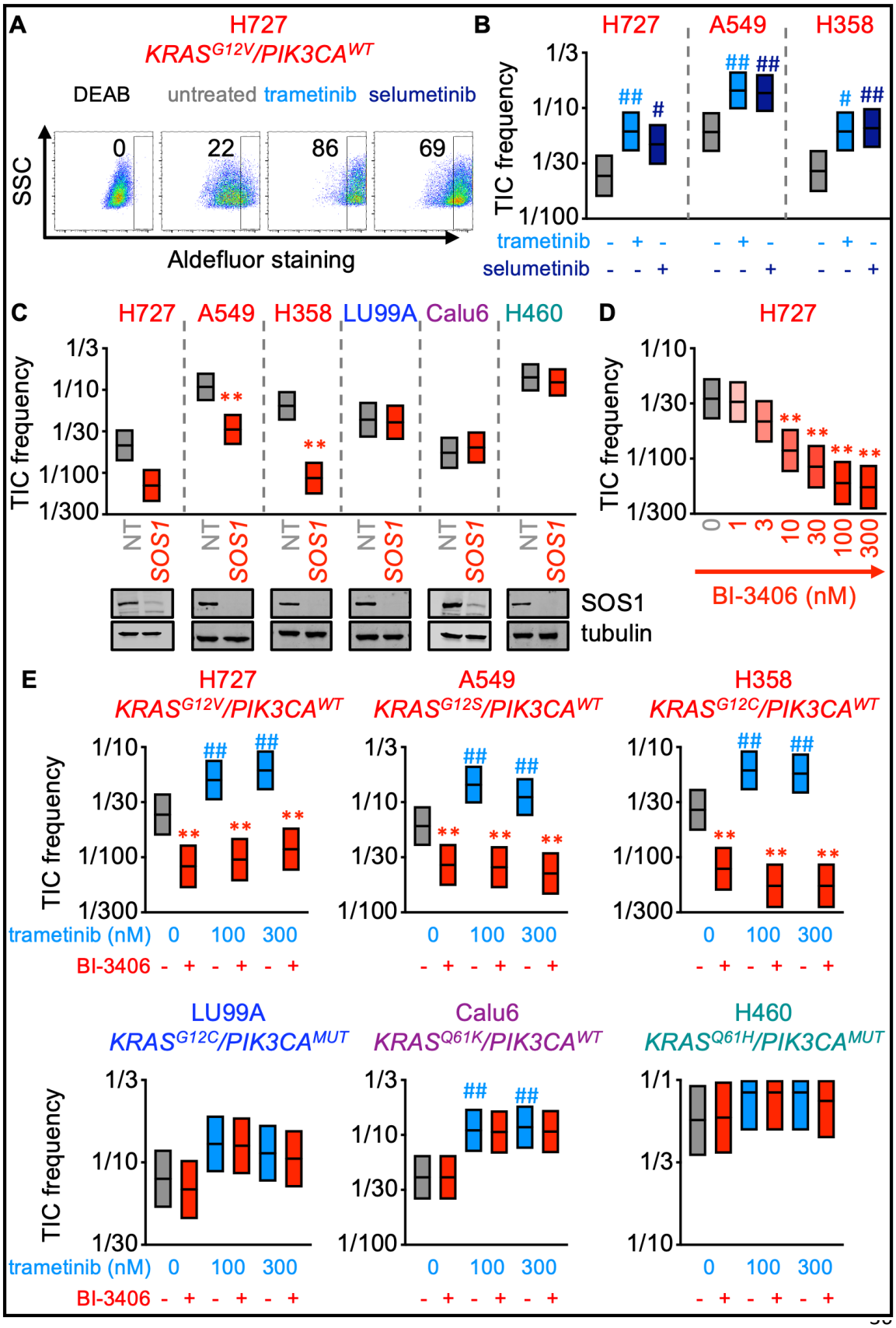
A
H727
KRASG12V/PIK3CAWT
DEAB
untreated
trametinib
selumetinib
SSC
Aldefluor staining
0
22
86
69
B
H727
A549
H358
TIC frequency
1/3
1/10
1/30
1/100
##
#
trametinib
selumetinib
C
H727
A549
H358
LU99A
Calu6
H460
TIC frequency
1/300
**
NT
SOS1
SOS1
tubulin
D
H727
0
1
3
10
30
100
300
BI-3406 (nM)
E
H727
KRASG12V/PIK3CAWT
A549
KRASG12S/PIK3CAWT
H358
KRASG12C/PIK3CAWT
trametinib (nM)
BI-3406
LU99A
KRASG12C/PIK3CAMUT
Calu6
KRASQ61K/PIK3CAWT
H460
KRASQ61H/PIK3CAMUT
1/1

**Figure 2.** SOS1 inhibition prevents trametinib-induced TIC outgrowth.

**(A)** Aldefluor staining for ALDH enzyme activity in DEAB negative control (DEAB), untreated H727 cells, or H727 cells treated with 100 nM trametinib or selumetinib for 72 hours. **(B)** TIC frequency from *in situ* ELDAs of the indicated cell lines pre-treated with 100 nM trametinib or selumetinib for 72 hours. # $p < 0.05$ vs untreated; ## $p<0.01$ vs. untreated for TIC upregulation.

**(C)** TIC frequency from *in situ* ELDAs (top) and Western blotting of WCLs for SOS1 and tubulin in the indicated LUAD cell lines where *SOS1* has been knocked out vs. non-targeting controls. ** $p<0.01$ vs. untreated. **(D)** TIC frequency from *in situ* ELDAs of H727 cells treated with the indicated doses of BI-3406. **(E)** TIC frequency from *in situ* ELDAs of the indicated cell lines pre-treated with trametinib for 72 hours to upregulate TICs, and then left untreated or treated with BI-3406. # $p < 0.05$ vs untreated; ## $p<0.01$ vs. untreated for TIC upregulation by MEK inhibitor treatment vs. untreated controls. * $p < 0.05$ vs untreated; ** $p<0.01$ for TIC inhibition by BI-3406 treatment compared to untreated controls. Data are representative of three independent experiments.

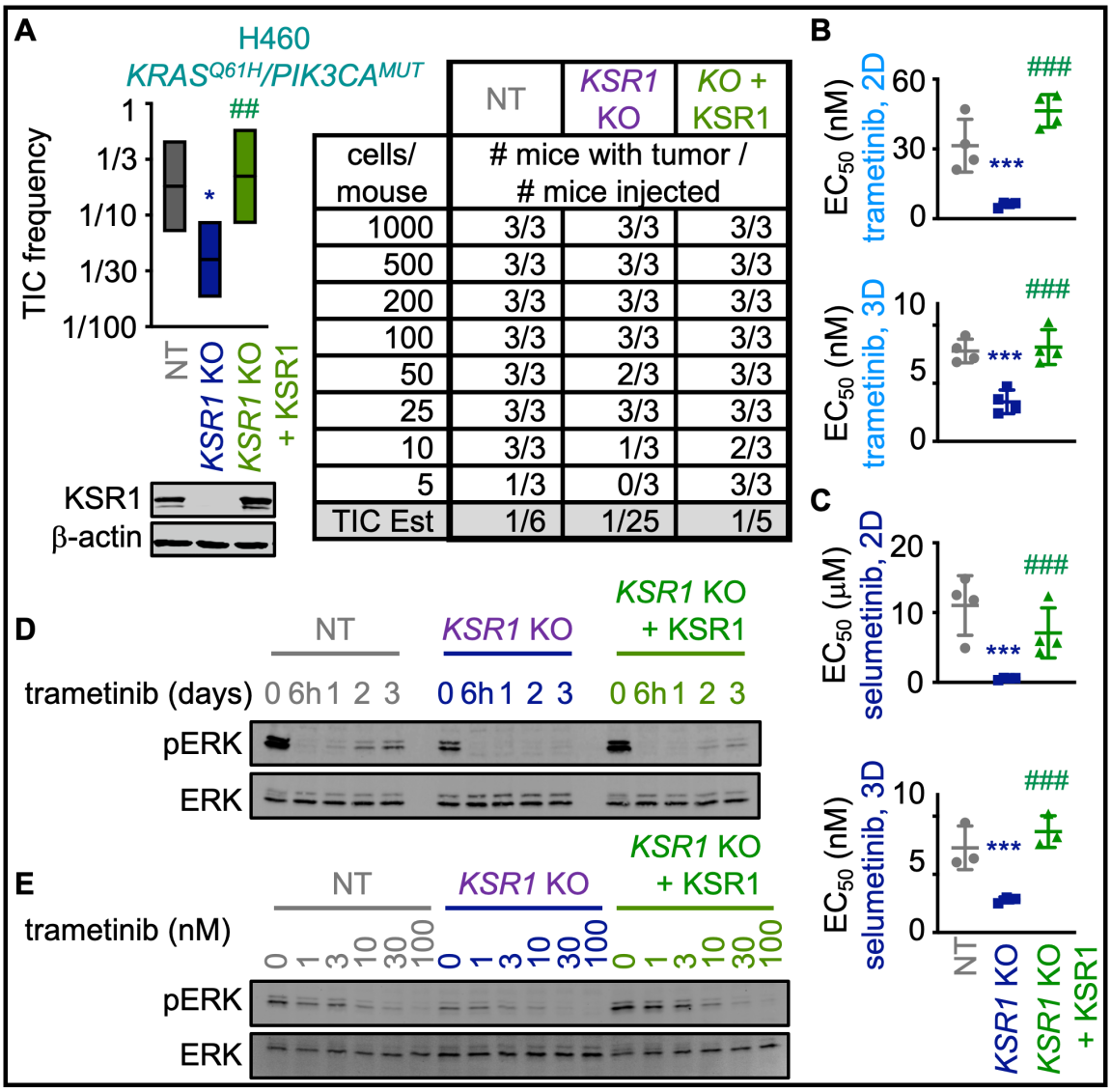


| cells/ mouse | NT # mice with tumor / # mice injected | *KSR1* KO | *KO* + KSR1 |
|---|---|---|---|
| 1000 | 3/3 | 3/3 | 3/3 |
| 500 | 3/3 | 3/3 | 3/3 |
| 200 | 3/3 | 3/3 | 3/3 |
| 100 | 3/3 | 3/3 | 3/3 |
| 50 | 3/3 | 2/3 | 3/3 |
| 25 | 3/3 | 3/3 | 3/3 |
| 10 | 3/3 | 1/3 | 2/3 |
| 5 | 1/3 | 0/3 | 3/3 |
| TIC Est | 1/6 | 1/25 | 1/5 |

**Figure 3.** *KSR1* KO inhibits tumor initiating cell (TIC) survival and enhances sensitivity to trametinib in *KRAS*-mutated LUAD genotypes.

**(A)** *In vivo* limiting dilution analysis data showing TIC frequency in H460 (*KRAS*$^{Q61H}$/*PIK3CA*$^{MUT}$) cells. The indicated numbers of cells were injected into the shoulder and flank of NCG mice (Charles River). Tumors were scored at 30 days. **(B-C)** $EC_{50}$ values for H460 cells treated with increasing concentrations of trametinib (B) or selumetinib (C) under anchorage-dependent (2D) or anchorage-independent (3D) conditions for 72 hours. Data are presented as mean ± s.d. from *N*=4 independent experiments. Western blots for KSR1 and β-actin in each cell population are shown in (A). **(D-E)** Western blots of WCLs H460 KSR1 KO an NT cells treated with trametinib (100 nM) for the indicated times (D) or with the indicated dose of trametinib for 24 hours (E). Western blots for pERK and ERK are representative from three independent

experiments. *p < 0.05; **** p<0.001 vs non-targeting controls; # p<0.05, ## p<0.01 vs. *KSR1* KO.

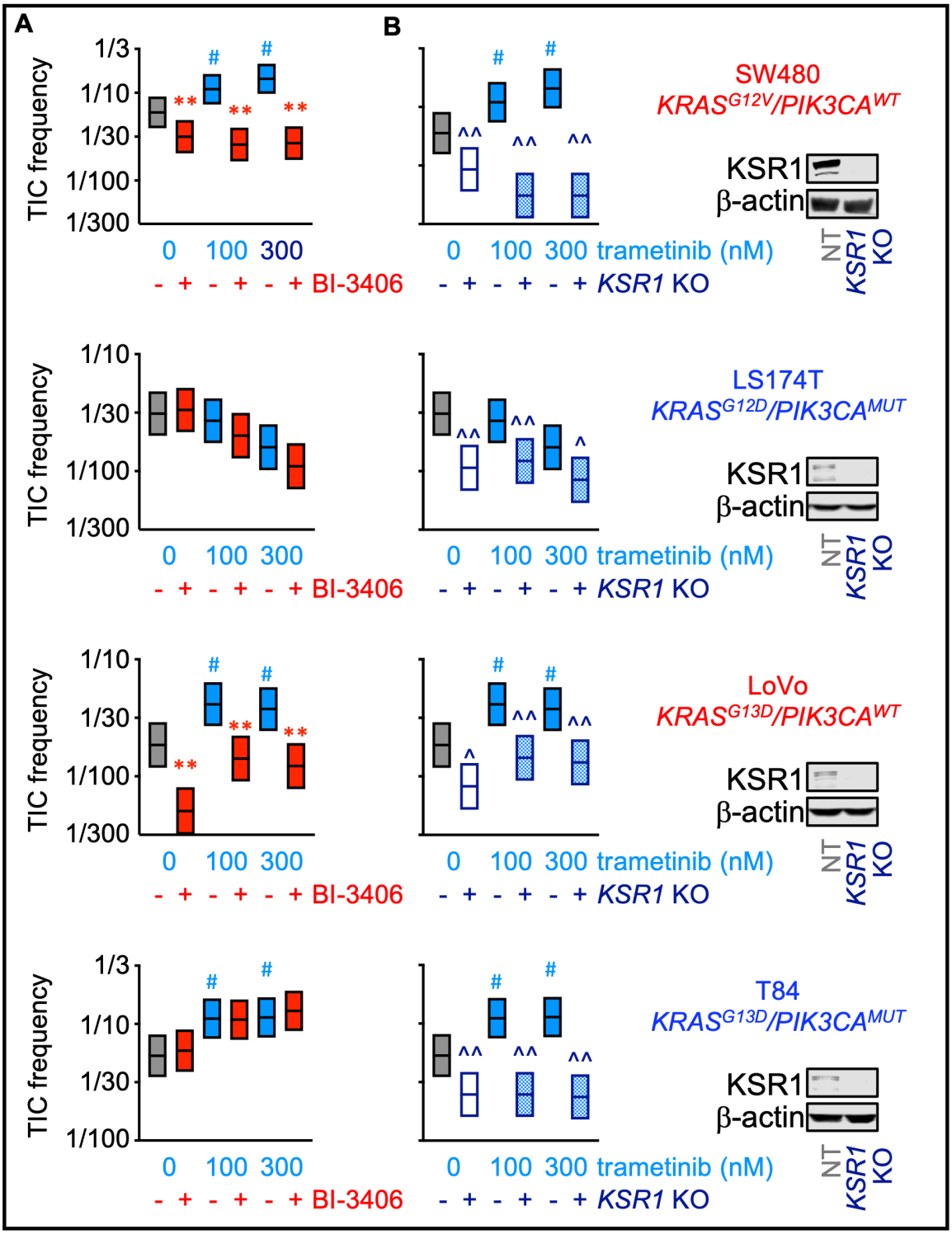


**Figure 4.** *KSR1* KO and SOS1 inhibition show differential inhibition of basal and trametinib-induced TICs in *KRAS*-mutated COAD cells.

**(A)** TIC frequency from *in situ* ELDAs in the indicated COAD cell lines pre-treated with trametinib for 72 hours to upregulate TICs, and then left untreated or treated with the SOS1 inhibitor BI-3406. The *KRAS* and *PIK3CA* mutational status for each cell line is indicated. **(B)** TIC frequency from *in situ* ELDAs in the indicated NT and *KSR1* KO COAD cells pre-treated with trametinib for 72 hours. Western blots of WCLs for KSR1 and β-actin are shown on the right. # $p < 0.05$ vs untreated; ## $p<0.01$ vs. untreated for TIC upregulation by MEK inhibitor treatment vs. untreated controls. ** $p<0.01$ for TIC inhibition by BI-3406 treatment compared to untreated controls. ^ $p< 0.05$; ^^ $p< 0.01$ for *KSR1* KO compared to untreated controls. Data are representative of three independent experiments.

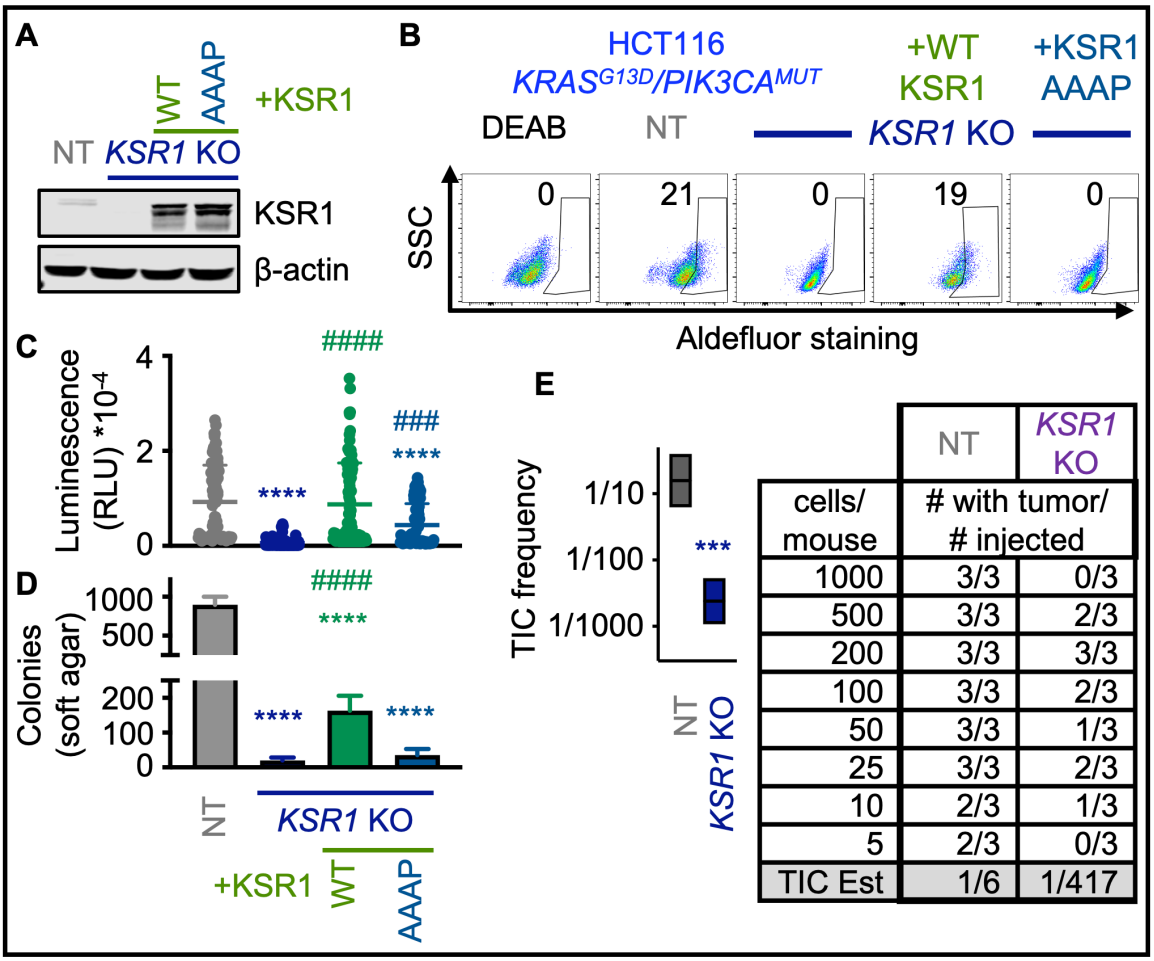


| cells/ mouse | NT # with tumor/ # injected | KSR1 KO # with tumor/ # injected |
|---|---|---|
| 1000 | 3/3 | 0/3 |
| 500 | 3/3 | 2/3 |
| 200 | 3/3 | 3/3 |
| 100 | 3/3 | 2/3 |
| 50 | 3/3 | 1/3 |
| 25 | 3/3 | 2/3 |
| 10 | 2/3 | 1/3 |
| 5 | 2/3 | 0/3 |
| TIC Est | 1/6 | 1/417 |

**Figure 5.** KSR1 regulation of TICs in COAD is dependent on interaction with ERK and relevant *in vivo*.

**(A)** Western blot for KSR1 and β-actin loading controls from WCLs HCT116 (*KRAS*$^{G13D}$/*PIK3CA*$^{MUT}$ NT, *KSR1* KO, *KSR1* KO + *KSR1* addback, and *KSR1* KO+ERK-binding mutant KSR1 (KSR1$^{AAAP}$) addback cells. **(B)** Aldefluor staining for ALDH enzyme activity in the indicated cells including a DEAB negative control. Data are representative from three independent experiments. **(C)** Single cell colony forming assays. Cells were single cell plated in non-adherent conditions, and colony formation was scored at 14 days by CellTitre Glo. Each individual point represents a colony. **(D)** Soft agar colony forming assay. $1 \times 10^3$ cells per well were plated in 0.4% agar, and colony formation was scored at 14 days. Data are presented as mean ± s.d. **(E)** *In vivo* limiting dilution analysis data showing frequency of TICs in Non-targeting Control (NT) and KSR1 KO HCT116 COAD cells. The indicated numbers of cells were injected into the shoulder and flank of NCG mice (Charles River). Tumors were scored at 30 days.

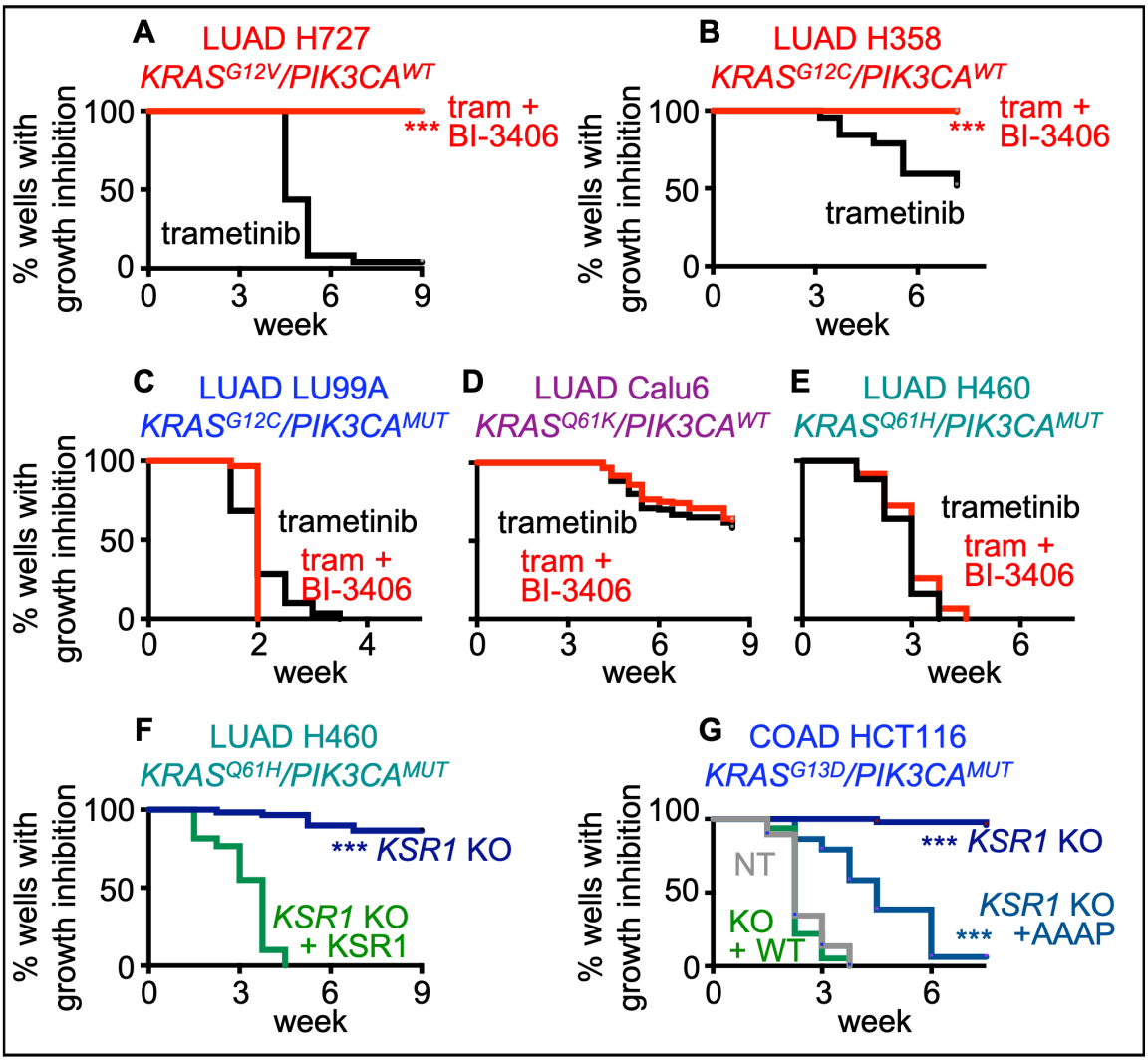


**Figure 6.** SOS1 inhibition and *KSR1* KO delay outgrowth of trametinib-resistant cells in multi-well resistance assays depending upon the KRAS mutational status.

Multi-well resistance assay were performed as outlined in the Materials and Methods. **(A-E).** Trametinib resistance in *KRAS*$^{G12X}$/*PIK3CA*$^{WT}$ H727 **(A)** and H358 **(B),** *KRAS*$^{G12X}$/*PIK3CA*$^{MUT}$ LU99A **(C),** *KRAS*$^{Q61X}$/*PIK3CA*$^{WT}$ Calu6 cells treated with trametinib **(D),** or *KRAS*$^{Q61X}$/*PIK3CA*$^{WT}$ H460 cells **(E)** treated with an $EC_{85}$ dose of trametinib with and without SOS1 inhibitor BI-3406. **(F-G).** Trametinib resistance in control and *KSR1* KO *KRAS*$^{Q61K}$-mutated/*PIK3CA*$^{MUT}$ H460 LUAD cells **(F)** and *KRAS*$^{G13D}$-mutated/*PIK3CA*$^{MUT}$ HCT116 COAD cells **(G).** In **G**, the expression of WT KSR1 and ERK-binding mutant KSR1$^{AAAP}$ transgenes on in *KSR1* KO trametinib sensitivity was also tested. Data from *N*=3 independent experiments were combined to generate Kaplan-Meier curves. *** $p<0.001$ vs single drug treatment (A-E) or NT controls (F-G).